

Silicide formation with codeposited titanium-tantalum alloys on silicon

C. D. Capiro, D. S. Williams, and S. P. Murarka

Citation: [Journal of Applied Physics](#) **62**, 1257 (1987); doi: 10.1063/1.339678

View online: <http://dx.doi.org/10.1063/1.339678>

View Table of Contents: <http://scitation.aip.org/content/aip/journal/jap/62/4?ver=pdfcov>

Published by the [AIP Publishing](#)

Articles you may be interested in

[A study of nitrogen behavior in the formation of Ta/TaN and Ti/TaN alloyed metal electrodes on SiO₂ and HfO₂ dielectrics](#)

Appl. Phys. Lett. **104**, 143501 (2014); 10.1063/1.4870338

[Silicide formation in the Ta/Ti/Si system by reaction of codeposited Ta and Ti with Si \(100\) and Si \(111\) substrates](#)

J. Appl. Phys. **85**, 1531 (1999); 10.1063/1.369283

[Furnace gas-phase chemistry of silicon oxynitridation in N₂O](#)


Appl. Phys. Lett. **68**, 1696 (1996); 10.1063/1.115909

[Alloy formation energetics and dynamics in the Ni/Cu\(100\) and Ni/Cu\(111\) systems](#)

J. Vac. Sci. Technol. A **10**, 2396 (1992); 10.1116/1.577972

[Interfacial reactions on annealing molybdenum-silicon multilayers](#)

J. Appl. Phys. **65**, 474 (1989); 10.1063/1.343425

**SHIMADZU**
Excellence in Science

Powerful, Multi-functional UV-Vis-NIR and FTIR Spectrophotometers

Providing the utmost in sensitivity, accuracy and resolution for applications in materials characterization and nano research

- Photovoltaics
- Polymers
- Thin films
- Paints
- Ceramics
- DNA film structures
- Coatings
- Packaging materials

[Click here to learn more](#)

A row of four Shimadzu spectrophotometers. From left to right: a small benchtop model, a larger benchtop model with a sample compartment, a large floor-standing model with a large sample compartment, and a large floor-standing model with a large sample compartment and a control panel.

Silicide formation with codeposited titanium-tantalum alloys on silicon

C. D. Capio and D. S. Williams

AT&T Bell Laboratories, 600 Mountain Avenue, Murray Hill, New Jersey 07974

S. P. Murarka

Department of Materials Engineering, Center for Integrated Electronics, Rensselaer Polytechnic Institute, Troy, New York 12180

(Received 5 January 1987; accepted for publication 21 April 1987)

The formation of disilicides of titanium and tantalum from Ti-Ta alloys codeposited on silicon and polycrystalline silicon have been investigated using x-ray diffraction techniques, resistance measurements, and Auger electron spectroscopy. Titanium and tantalum in the Ti-Ta alloy interacted independently with silicon. There was no titanium/tantalum compound formation and no ternary was detected. The growth of each metal silicide was sustained by continuous out-diffusion of silicon into the Ti-Ta alloy film until the metals were consumed in the silicide transformation. This behavior may account for the absence of phase separation and component accumulation. An initial reaction was observed after the 600 °C, 30 min anneal. The stable end phases formed at temperatures ≥ 800 °C are TiSi_2 and TaSi_2 . High molecular weight intermetallics such as Ta_5Si_3 and Ti_5Si_3 that are normally not detected in Ta-Si and Ti-Si interaction studies were detected, suggesting a stabilizing effect of the impurities. The sheet resistance of the heat-treated samples is: (a) a strong function of the titanium content of the Ti-Ta alloy (low for Ti-rich alloys); (b) lower on silicon substrates; (c) invariant at temperatures > 900 °C. The etch rate of the heat-treated samples in buffered hydrofluoric acid increased with increasing titanium content in the film.

I. INTRODUCTION

Silicides of tantalum and titanium metals have found increasing applications in the VLSI silicon device technology because of their inherently low bulk resistivity, the ease with which they are formed, and their high-temperature stability.¹⁻⁴ Tantalum disilicide has a resistivity which ranges from 35–45 $\mu\Omega$ cm, can stand up to HF-containing solutions, and can withstand high-temperature processing > 900 °C. Titanium disilicide has a resistivity of < 15 $\mu\Omega$ cm, promises wide applications to VLSI device technology including its use as a self-aligned contact metallization,⁵ and is also stable at temperatures > 900 °C.

While the low resistivity and high-temperature stability of TiSi_2 makes it potentially attractive for the gate and interconnect metallization of MOS devices, it has one disadvantage—its high solubility in HF-containing solutions. An approach for alleviating this problem is to employ a composite structure in which TiSi_2 is formed at the silicon interface with an HF-resistant disilicide as the outer layer. Studies^{3,6,7} on the reaction of alloys and bilayers of transition metals with silicon have shown that annealing leads to the formation of a single metal silicide at the silicon interface together with a mixed or uniform silicide structure in the outer surface region in a layered fashion.⁶ By cosputtering titanium-tantalum alloys on silicon, followed by a heat treatment at 700 °C or higher temperature, a layered structure with the TiSi_2 formed at the silicon interface and TaSi_2 as the surface layer was though possible. We have chosen the Ti-Ta system because the separate behavior of these transition metals has already been investigated^{8,9} and their stable silicides, TaSi_2 and TiSi_2 , are currently used in VLSI silicon device technology.

This paper describes our study of the formation and properties of the silicides in the Ti-Ta-Si system. The Ti-Ta

alloys of various compositions were codeposited on single-crystal silicon (silicon) and on polycrystalline silicon (hereafter called polysilicon) substrates. The silicide formation has been studied on annealed samples using x-ray diffraction techniques, resistance measurements, etch rate measurements in buffered hydrofluoric acid (BHF) solutions, and Auger electron spectroscopy (AES).

II. EXPERIMENT

7.5-cm-diam, *n*-type (100) phosphorous-doped wafers with resistivity of 3–10 Ω cm were used in these studies. The wafers were dipped into 100:1 ($\text{H}_2\text{O}:\text{HF}$), rinsed in deionized (DI) water for 2 min, and spin-dried before loading into the film deposition chamber. Polysilicon samples were prepared by oxidizing silicon wafers in dry oxygen to form 1000 Å of the oxide and then depositing 4000 Å of polysilicon by low-pressure chemical vapor deposition (LPCVD). The films were then deposited with phosphorus using PBr_3 at 950 °C for 60 min. The metal alloy films were codeposited in a Magnetron S-gunTM system in argon using two high-purity targets, one tantalum and the other titanium. The thickness and composition of the films were determined by the use of deposition parameters.¹⁰ The alloy compositions prepared were $\text{Ti}_{10}\text{Ta}_{90}$ and $\text{Ti}_{50}\text{Ta}_{50}$ on silicon and polysilicon substrates with a film thickness of 1000 Å. In a typical deposition, the chamber was evacuated to 10^{-7} Torr and then argon was bled in. The plasma was started and the power adjusted with the shutter closed. After 3 min the deposition was started by opening the shutter. For the $\text{Ti}_{50}\text{Ta}_{50}$ depositions the rf power settings were 500 and 275 W for the Ti and Ta targets, respectively, for a 12-min deposition. For the $\text{Ti}_{10}\text{Ta}_{90}$ depositions, the rf power settings were 126 and 760 W, respectively, for a 9-min deposition. All the wafers were deposited with a dc bias at 40 V. The samples on polysilicon

TABLE I. Designation of experimental structures.

Sample no.	Alloy/Substrate
1	Ti ₁₀ Ta ₉₀ /silicon
2	Ti ₁₀ Ta ₉₀ /polysilicon
3	Ti ₅₀ Ta ₅₀ /silicon
4	Ti ₅₀ Ta ₅₀ /polysilicon

and on silicon were numbered as shown in Table I.

The samples were annealed in a vacuum at various temperatures from 500–900 °C. The annealing times varied from 30 to 120 min. Anneals were performed in a 9-ft-long stationary quartz tube with a Lindberg resistance furnace mounted on a Velmex track so that it can be moved along the tube. Typically, the samples were inserted into the cold zone of the furnace tube and then the tube was evacuated. When the pressure reached approximately 10^{-7} Torr, the hot furnace was moved over the samples. After the heat treatment, the furnace was moved back to allow the samples to cool at the same pressure prior to backfilling with nitrogen.

Identification of the reaction products was made using x-ray diffraction techniques. The sheet resistance measurements were made using a four-point probe and Auger electron spectroscopy was used to determine the component concentration profiles. For film thickness measurements, a step was made on the film to be measured by masking a portion of that film with a piece of electroplaters tape. The taped sample was dipped into buffered (30:1) hydrofluoric acid for a set time, rinsed in water and then spin dried. The step was measured using the Sloan DEKTAK.TM

III. RESULTS

A. X-ray studies

The cosputtered films of Ti-Ta alloys were amorphous in the as-deposited state. Figures 1–4 show the diffraction patterns of the samples after annealing in vacuum for 30 min at the indicated temperatures. The intensities of all reflections are expressed relative to the maximum intensity peak of each individual sample. A summary of the results of the x-ray studies is presented in Table II. The intensities of selected reflections for the samples were plotted as a function of the annealing temperatures in Figs. 5–8.

1. Ti₁₀Ta₉₀ alloy

Figure 1 shows the x-ray diffraction pattern for the samples of Ti₁₀Ta₉₀ alloy codeposited on silicon substrates annealed at the indicated temperatures. As-deposited, the sample exhibited a very broad peak centered at $2\theta = 33^\circ$. Following a 500 °C heat treatment, five reflections appeared that matched those of tantalum, titanium, and an intermediate silicide, Ta₅Si₃. This high molecular weight intermetallic phase of Ta is known⁸ to form at low temperatures, $<700^\circ\text{C}$, where $\text{Si}/\text{Ta} < 1$. Following the 600 °C anneal, weak Bragg reflections of TiSi were detected. This result indicated that an initial reaction occurred at some temperature between 500 and 600 °C. The appearance of some new diffraction lines which correspond with the reflections of tantalum disilicide and other intermetallic phases of titanium silicides were observed after the 700 °C anneal. At temperatures $\geq 800^\circ\text{C}$ tantalum disilicide and titanium disilicide were found to be the dominant phases.

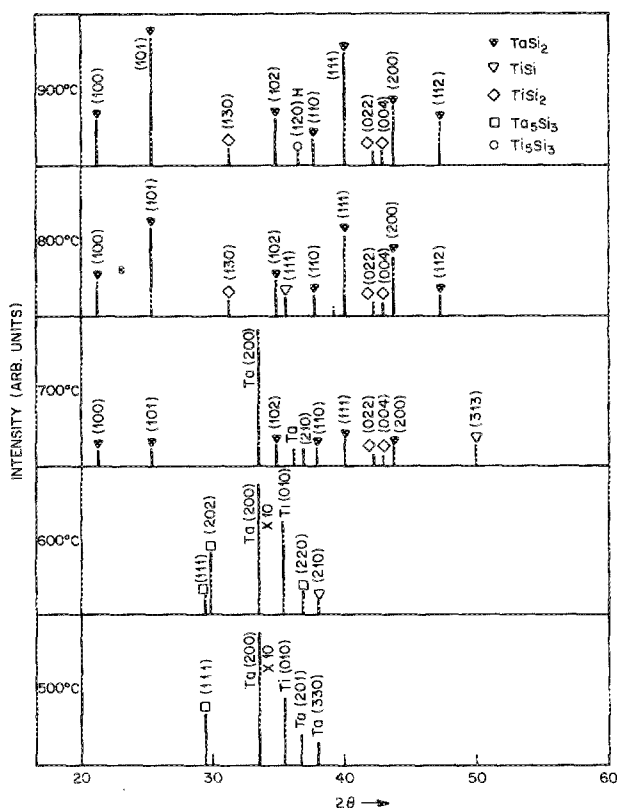


FIG. 1. X-ray diffraction pattern of Ti₁₀Ta₉₀/silicon annealed in vacuum for 30 min at the temperatures indicated.

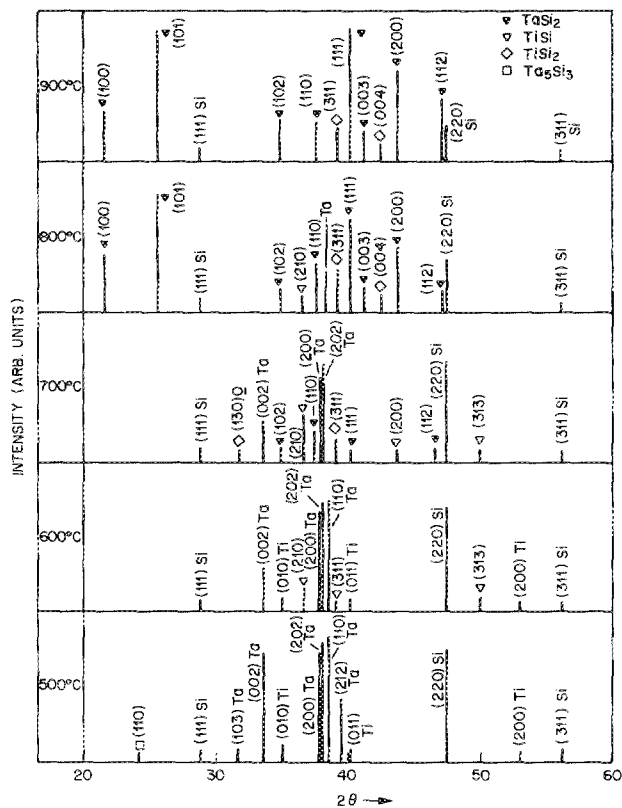


FIG. 2. X-ray diffraction pattern of Ti₁₀Ta₉₀/polysilicon annealed in vacuum for 30 min at the temperatures indicated.

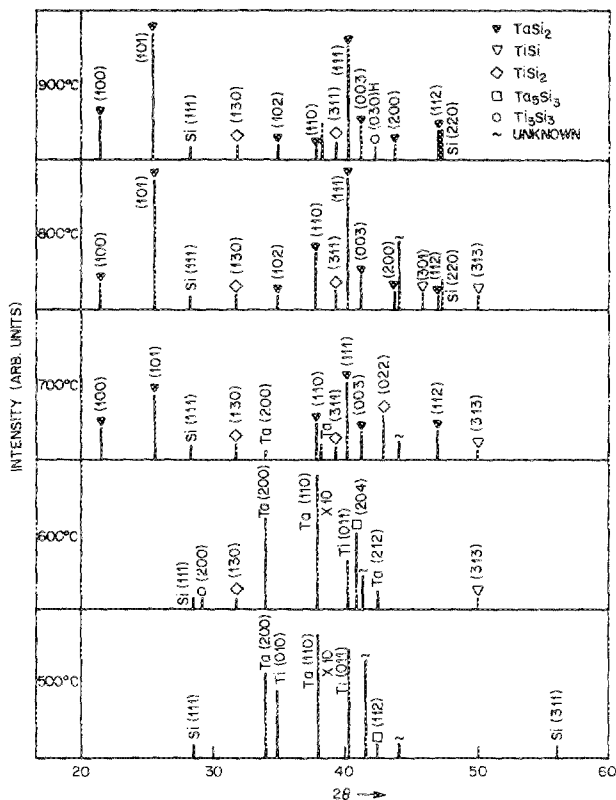


FIG. 3. X-ray diffraction pattern of $\text{Ti}_{50}\text{Ta}_{50}$ /silicon annealed in vacuum for 30 min at the temperatures indicated.

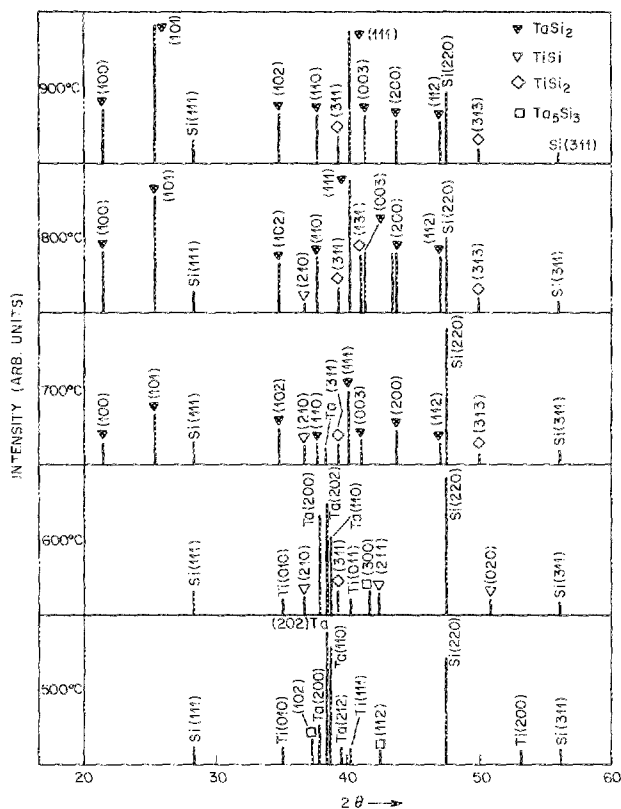


FIG. 4. X-ray diffraction pattern of $\text{Ti}_{50}\text{Ta}_{50}$ /polysilicon annealed in vacuum for 30 min at the temperatures indicated.

TABLE II. Summary of x-ray results.

Alloy composition	Substrate	Heat treatment data		
		Temp. (°C)	Time (min)	Intermetallic phases observed
$\text{Ti}_{50}\text{Ta}_{50}$	Si	500	30	Ta_5Si_3
		600	30	Ta_5Si_3 , TiSi
		700	30	TaSi_2 , TiSi, TiSi ₂
		800	30	TaTi_2 , TiSi, TiSi ₂
		900	30	TaSi_2 , Ti ₃ Si ₃ , TiSi ₂
	polySi	500	30	Ta_5Si_3
		600	30	TiSi
		700	30	TaSi_2 , TiSi, TiSi ₂
		800	30	TaSi_2 , TaSi, TiSi ₂
		900	30	TaSi_2 , TiSi ₂
$\text{Ti}_{10}\text{Ta}_{90}$	Si	500	30	Ta_5Si_3
		600	30	TiSi, Ti ₃ Si ₃ , TiSi ₂
		700	30	TaSi_2 , TiSi, TiSi ₂
		800	30	TaSi_2 , TiSi, TiSi ₂
		900	30	TaSi_2 , Ti ₃ Si ₃ , TiSi ₂
	polySi	500	30	Ta_5Si_3
		600	30	Ta_5Si_3 , TiSi, TiSi ₂
		700	30	TaSi_2 , TiSi, TiSi ₂
		800	30	TaSi_2 , TiSi ₂
		900	30	TaSi_2 , TiSi ₂
$\text{Ti}_{50}\text{Ta}_{50}$	Si	900	12.0	Ta_5Si_3 , TaSi_2 , Ti ₃ Si ₃ , TiSi ₂
$\text{Ti}_{10}\text{Ta}_{90}$	Si	900	120	Ta_5Si_3 , TaSi_2 , TiSi ₂

As can be seen in Fig. 5, titanium was consumed rapidly and was no longer detected at 700 °C. The tantalum peak intensity decreased rapidly after 600 °C and was no longer detected at 800 °C. TaSi_2 and TiSi_2 were first detected following the 700 °C anneal. Their peak intensities reached a maximum at 800 °C and no further change was observed at temperatures > 800 °C.

The x-ray diffraction pattern of the $\text{Ti}_{10}\text{Ta}_{90}$ alloy codeposited on polysilicon, shown in Fig. 2, appears dissimilar to that of the sample alloy deposited on monosilicon shown in Fig. 1. The x-ray spectrum of the sample sintered at 500 °C

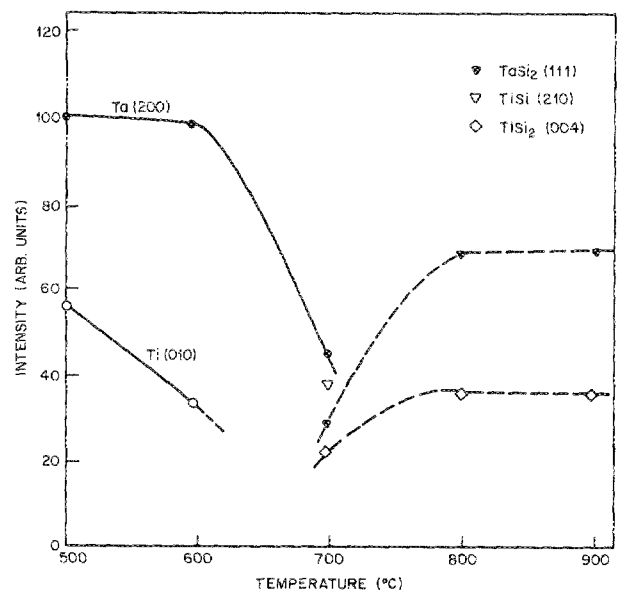


FIG. 5. X-ray diffraction intensity of selected reflections of $\text{Ti}_{10}\text{Ta}_{90}$ /silicon annealed in vacuum for 30 min as a function of annealing temperatures.

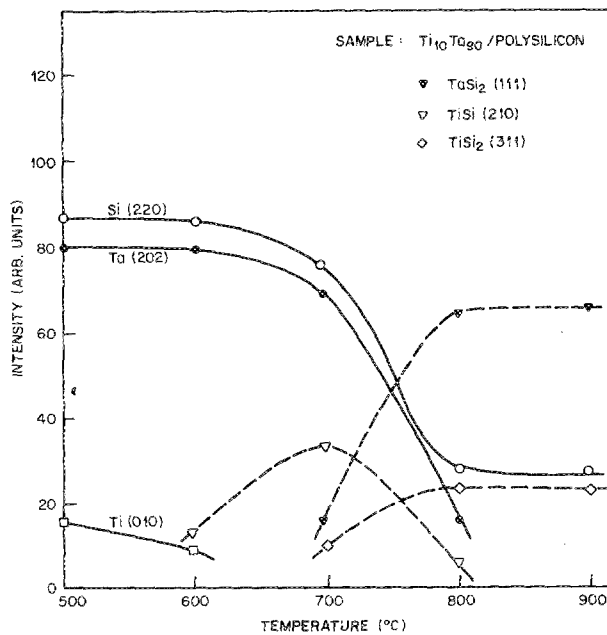


FIG. 6. X-ray diffraction intensity of selected reflections of $\text{Ti}_{10}\text{Ta}_{90}$ /poly-silicon annealed in vacuum for 30 min as a function of annealing temperatures.

shows an abundance of reflections of tantalum, titanium, and silicon. The cluster, centered about $2\theta = 38^\circ$, corresponds to the position of the tetragonal tantalum and the cubic tantalum-rich intermediate phase, Ta_5Si_3 . The reaction following anneals at higher temperatures gave the same results as the samples on single-crystal silicon.

In Fig. 9, the AES depth profile of $\text{Ti}_{10}\text{Ta}_{90}$ /polysilicon, following anneal at 500°C , exhibits a uniform distribution of tantalum and titanium throughout the thickness of the alloy with no evidence of reaction with the polysilicon substrate. An accumulation of oxygen and carbon were found on the

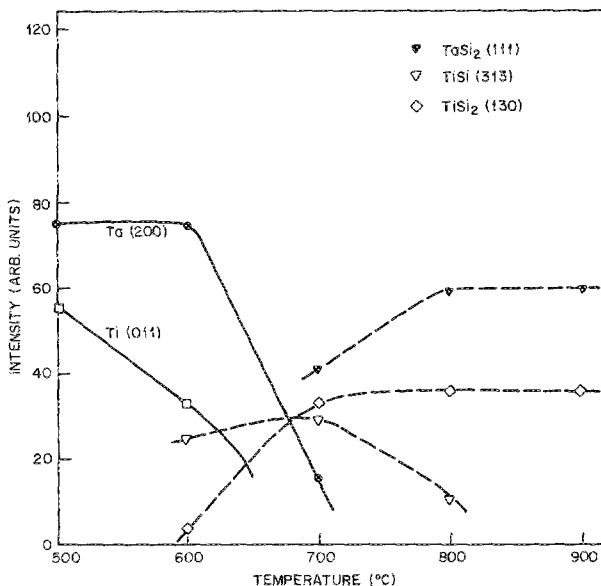


FIG. 7. X-ray diffraction intensity of selected reflections of $\text{Ti}_{50}\text{Ta}_{50}$ /silicon annealed for 30 min as a function of annealing temperatures.

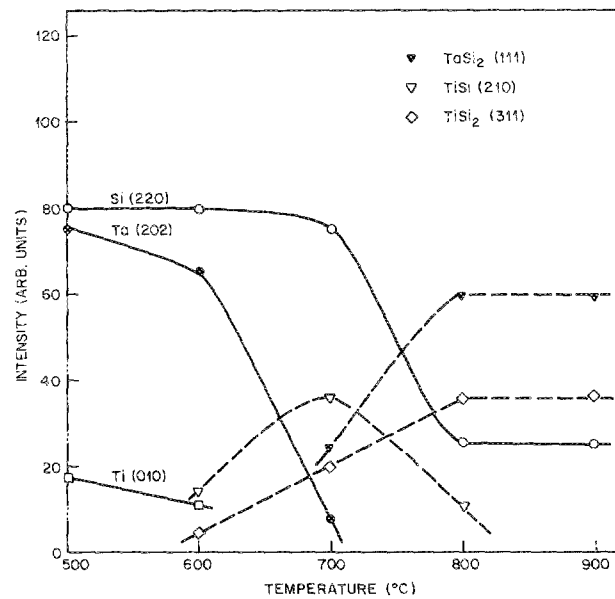


FIG. 8. X-ray diffraction intensity of selected reflections of $\text{Ti}_{50}\text{Ta}_{50}$ /poly-silicon annealed for 30 min as a function of annealing temperatures.

surface. In addition there is small amount of oxygen in the film, the origin of which has not been determined.

In Fig. 6, the intensity of the titanium peaks decreased rapidly and was no longer detected after annealing at 700°C . The tantalum and silicon (polysilicon) intensities decreased slowly as the annealing temperature was raised to 700°C and then the intensities decreased rapidly upon annealing at 800°C . No tantalum was detected at 900°C and no further decrease of the silicon peak intensity was observed. The x-ray intensities of both the TaSi_2 and the TiSi_2 reflections increased at 800°C with no further increase observed at higher temperatures.

In Fig. 10, the AES depth profile of this sample, after annealing at 900°C , reveals a uniform distribution of reaction products with no evidence of a layered structure nor of oxygen contamination. About 40% of the polysilicon was consumed in the silicide formation.

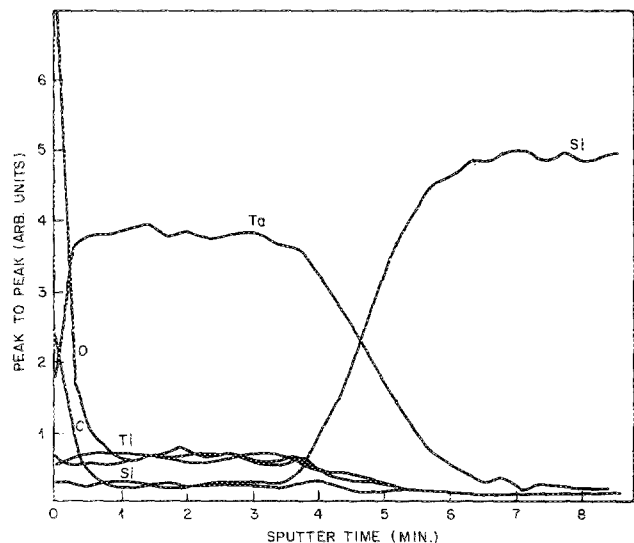


FIG. 9. AES depth profile of $\text{Ti}_{10}\text{Ta}_{90}$ /polysilicon following anneal at 500°C for 30 min.

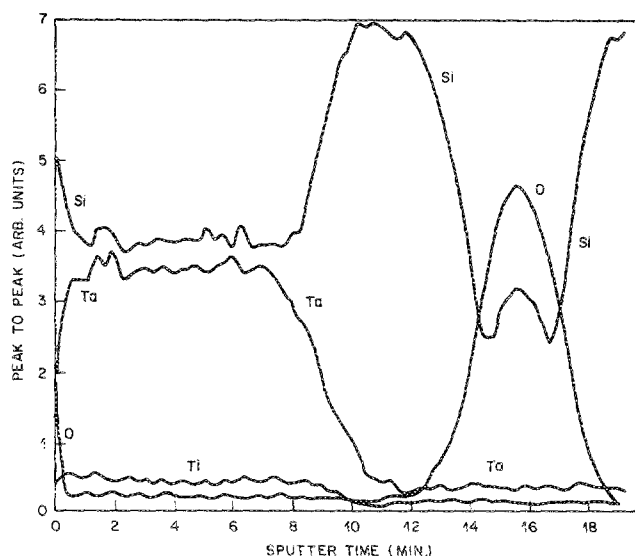


FIG. 10. AES depth profile of $\text{Ti}_{10}\text{Ta}_{90}$ /polysilicon following anneal at 900°C for 30 min.

2. $\text{Ti}_{50}\text{Ta}_{50}$ alloy

Figure 3 shows the x-ray diffraction pattern of the $\text{Ti}_{50}\text{Ta}_{50}$ alloy codeposited on silicon samples following heat treatment at various temperatures. Following the 500°C anneal, some very strong peaks of tantalum and titanium and a weak peak that matches the reflection of Ta_5Si_3 were detected. After the 600°C anneal, a peak of TiSi and a weak peak of TiSi_2 were detected. At 900°C , the x-ray spectrum consists of strong peaks of TaSi_2 , TiSi_2 , Si, and a weak peak that matches the reflection of hexagonal Ti_5Si_3 .

In Fig. 7, the intensity of the tantalum peak decreased rapidly after annealing at 600°C . After 700°C , a very small amount of tantalum was still detected. No tantalum was detected at 800°C . For temperatures $\geq 700^\circ\text{C}$, no further change was observed except the change in the TiSi line intensity which decreased at 800°C and was not seen after the 900°C anneal.

Figure 4 shows the x-ray diffraction pattern of the same alloy on polysilicon after various heat treatments. Following a 500°C anneal, strong peaks of tantalum, titanium, silicon, and two weak peaks of Ta_5Si_3 were detected. Reaction at higher temperatures for this sample produced results similar to those obtained from the samples described earlier, with TiSi_2 and TaSi_2 being the dominant end phases at temperatures $\geq 800^\circ\text{C}$.

The AES profile of the $\text{Ti}_{50}\text{Ta}_{50}$ /polysilicon after a 500°C anneal is shown in Fig. 11. Note the uniform distribution of the tantalum and titanium with no apparent interdiffusion indicative of phase separation. An appreciable amount of oxygen was incorporated in the alloy during the anneal, possibly due to a leak in the annealing system. The accumulation of oxygen and carbon was found to be high in the surface region.

As can be seen in Fig. 8, the tantalum peak intensity decreased more rapidly than the titanium intensity for annealing temperatures $\leq 600^\circ\text{C}$. Following a 700°C anneal, no titanium was detected and the tantalum intensity was greatly diminished. The intensity of the polysilicon diffrac-

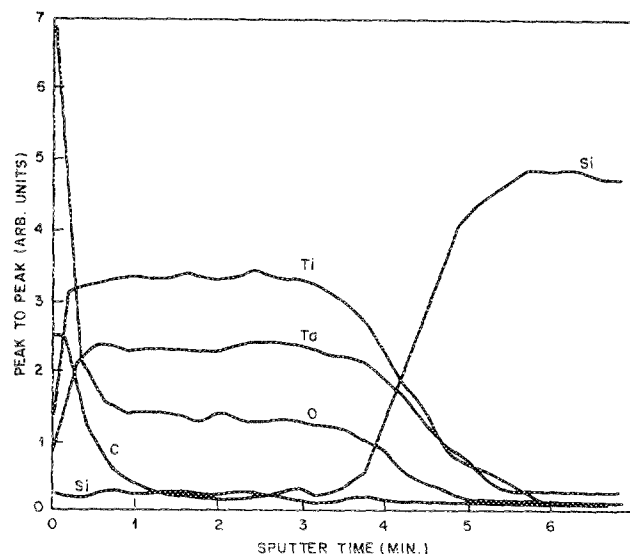


FIG. 11. AES depth profile of $\text{Ti}_{50}\text{Ta}_{50}$ /polysilicon following a 500°C anneal for 30 min.

tion line decreased rapidly at temperatures from 700 to 800°C . No further decrease occurred at higher annealing temperatures. As seen in Fig. 7, TiSi is detectable after 800°C anneal but not after 900°C .

The Auger profile of the sample after the 900°C anneal is shown in Fig. 12. No oxygen and carbon are seen in the bulk of the film. However, there is an accumulation of carbon on the surface and oxygen just underneath this carbon contaminated layer. The carbon accumulation near the surface region inhibited the tantalum reaction while it aided the titanium reaction. Oxygen appeared to have inhibited the titanium reaction while it aided the tantalum reaction. These results are consistent with the observations of the Ta-W-Si (Ref. 6) and the Ti-Si (Ref. 9) systems where carbon has been shown to retard the tantalum silicide formation and oxygen has been shown to retard the titanium silicide formation. As for phase separation, none was evident. Silicides of

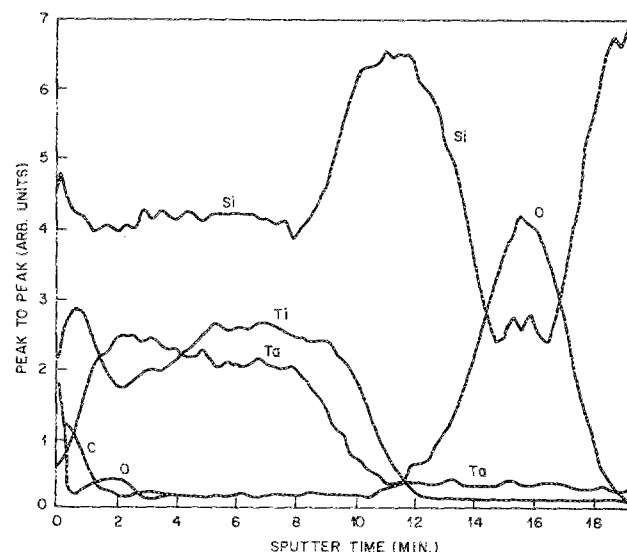


FIG. 12. AES depth profile of $\text{Ti}_{50}\text{Ta}_{50}$ /polysilicon following a 900°C anneal in vacuum for 30 min.

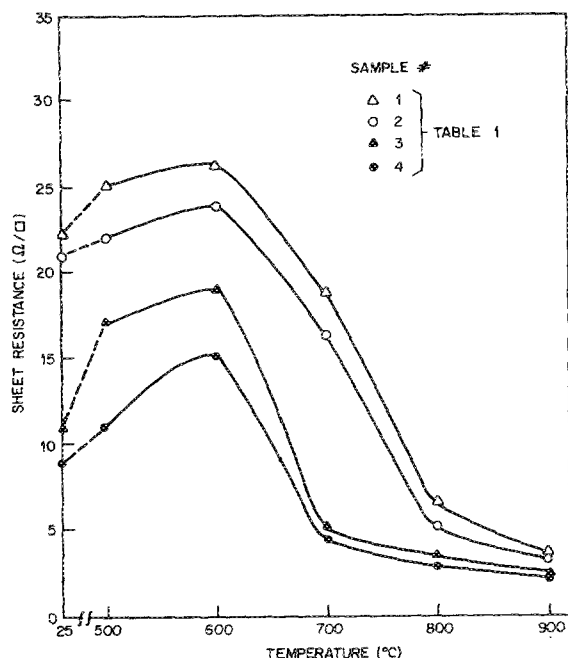


FIG. 13. Sheet resistance of various samples as a function of annealing temperatures in vacuum for 30 min.

titanium and tantalum can be found near the surface as well as the interface. About 40% of the polysilicon was consumed in the silicide formation.

B. Resistance measurements

The dependence of the sheet resistance on the annealing temperatures for the set of samples annealed for 30 min is shown in Fig. 13. The resistances before the heat treatments are also shown. The sheet resistance increased from the as-deposited value to a maximum at approximately 600 °C for all samples. This behavior of the sheet resistance correlates with the x-ray and AES observations. For example, the rise of resistivity to a maximum at approximately 600 °C is associated with the events occurring at this temperature and the possible contributions of oxygen and silicon diffusion into the alloy. The AES depth profile after the 500 °C anneal showed a small amount of oxygen and silicon. Oxygen and/or silicon incorporated in the film should increase its resistivity.⁹ The increase in resistivity is also associated with a decrease in the x-ray intensity of the titanium, tantalum, and silicon reflections. Very weak reflections of TiSi and TiSi₂ were detected clearly indicating that the initial reaction occurred at a temperature close to 600 °C.

From the maximum at 600 °C, the sheet resistance value decreased rapidly to near minimum value at 700 °C for the Ti₅₀Ta₅₀ samples and 800 °C for the Ti₁₀Ta₉₀. The low values of the sheet resistance of samples 3 and 4 (see Table I) reflect the high titanium content of the alloy. This would indicate that the sheet resistance is a strong function of the titanium content of the Ti-Ta alloy film.

Figure 14 shows a similar plot for samples annealed for 120 mins. For all samples, the maximum resistance was higher than the previous samples (Fig. 13) after annealing at the temperature of approximately 600 °C. The plots showed

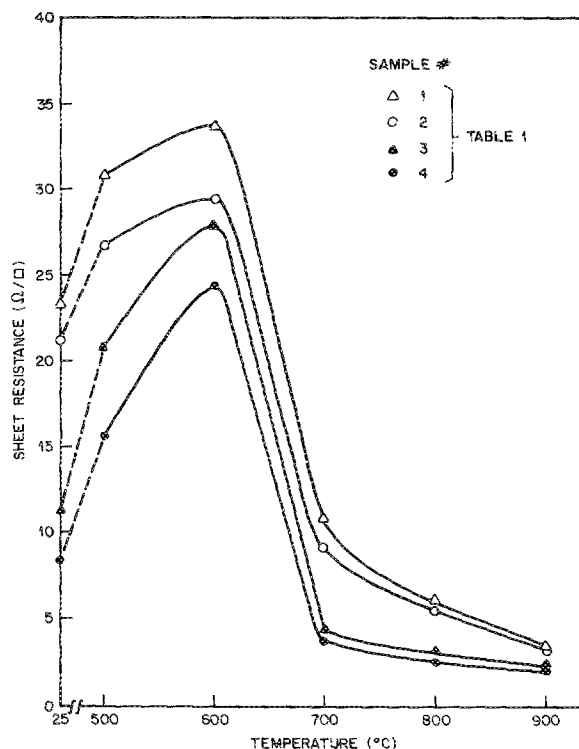


FIG. 14. Sheet resistance of various samples as a function of annealing temperatures in vacuum for 120 min.

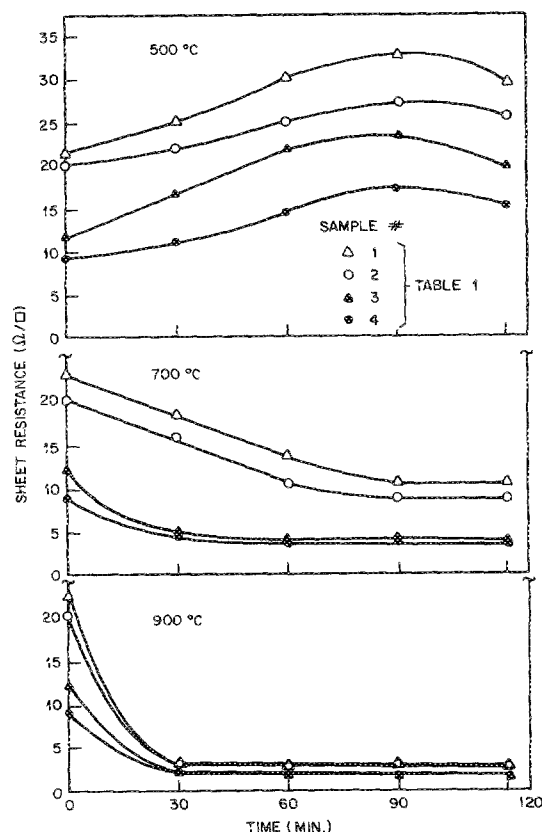


FIG. 15. Sheet resistance of various samples annealed at various temperatures as a function of time.

TABLE III. Chemical etch rate.^a

Ti ₅₀ Ta ₅₀ (annealed)	Etch rate (Å/min) of silicides on	
	Polysilicon	Silicon
900 °C/30 min	111.8	94.4
800 °C/30 min	85.9	37.4
700 °C/30 min	71.6	35.1
600 °C/30 min	35.6	21.0
500 °C/30 min	15.7	14.1
Ti ₁₀ Ta ₉₀ (annealed)		
900 °C/60 min	20.2	12.0
700 °C/30 min	5.0	3.5
500 °C/30 min	0.0	0.0
TiSi ₂ (CVD)	504.0	
TaSi ₂ (CVD)	5.1	
TiSi ₂ (Sputtered)	256.0	

^a Etchant: BHF (30% BOE): 30 parts ammonium fluoride 40% and 1 part hydrofluoric acid 49%.

the same increase-maximum-decrease behavior that was observed in the 30 min annealing, but differ slightly in their behavior above 600 °C. The sheet resistance of all samples decreased rapidly to a minimum at 700 °C. From 700 °C, samples 1 and 2 (see Table I) decreased in resistance at a moderate rate while samples 3 and 4 decreased only slightly. Ti-rich samples exhibited a lower final resistance. As can be seen in Figs. 13 and 14, alloy films codeposited on polysilicon substrates exhibited lower resistances than those on silicon substrates because of the contribution from the doped polysilicon film which has lower sheet resistance than the silicon substrate.

The effect of annealing time on the sheet resistance for three annealing temperatures (500, 700, and 900 °C) are shown in Fig. 15. At 500 °C, the resistance increased to a maximum in 90 mins. At 120 mins, the resistivity is lower

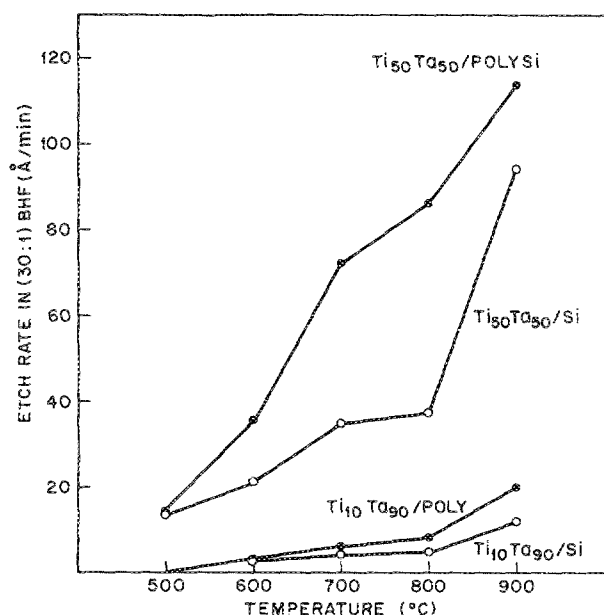


FIG. 16. Etch rate in (30:1)BHF as a function of silicide formation temperature.

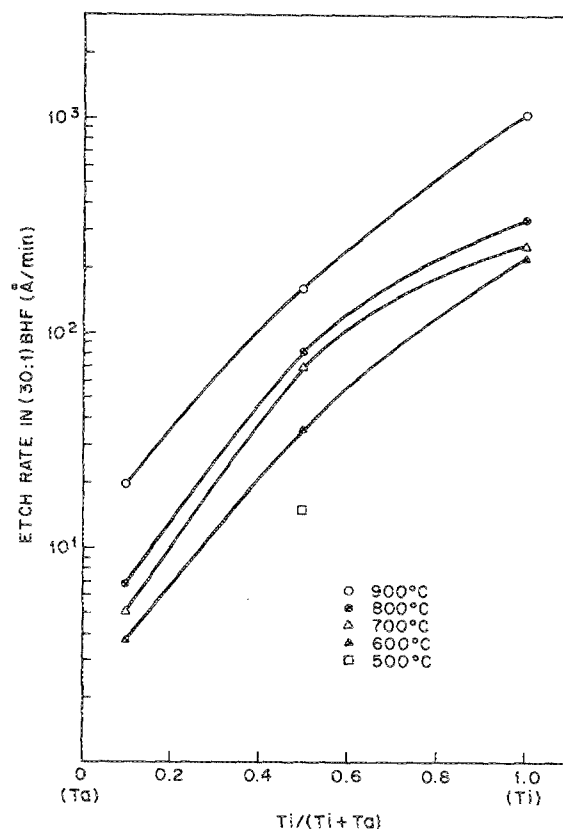


FIG. 17. Etch rate in (30:1)BHF as a function of alloy composition on polysilicon substrate.

than maximum but still higher than that at room temperature. At 700 °C, the sheet resistance reached a minimum value in 90 min for the Ti₁₀Ta₉₀ samples and only 30 min for the Ti₅₀Ta₅₀ samples. This rapid decrease may be explained by the appearance of both tantalum and titanium disilicide phases in the early stages of reaction with silicon at temperatures between 600 and 700 °C. The low-temperature reactivity of titanium with silicon has resulted in more titanium disilicide being formed. Under these conditions, the resistivity of the TiSi₂ from the Ti-rich sample would dominate. At 900 °C, the sheet resistance of all samples decreased to its minimum value in only 30 min. This behavior is associated with the x-ray diffraction results for anneals at 900 °C, 30 min, where the disilicides of titanium and tantalum dominated the x-ray diffraction spectrum.

C. Etch rate studies

The etch rate of the ternary alloys was measured to determine if the rate of material removal in buffered HF would reflect the changes in the compound formation indicated by the x-ray diffraction. The results of the etching experiments are shown in Table III. Figure 16 shows the etch rate as a function of the annealing temperatures for two different alloys deposited on silicon and on polysilicon. The etch rate increased with anneal temperature and was higher for films with more Ti. There were no discontinuities in etch rates at the temperatures where the appearance of abrupt changes in resistivities were observed. The etch rate behavior correlated with the decrease in the resistivity of the films annealed at

higher temperatures indicating that the increasing silicide contents lead to higher etch rates in BHF. Because TiSi_2 has a high dissolution rate in HF-bearing solutions, the rapid rise in the etch rate of the titanium-rich samples ($\text{Ti}_{50}\text{Ta}_{50}$) could be attributed to the higher TiSi_2 content of the film at all temperatures. The etch rates for both alloy compositions are higher for films formed on polysilicon than on silicon. This is possibly due to the presence of smaller grains on the polysilicon.

The etch rate versus composition curves for films deposited on polycrystalline silicon substrates are shown in Fig. 17. For the single-crystal substrates similar curves are obtained. The etch rates increase linearly with increasing Ti content of the alloy at all annealing temperatures.

As can be seen in Table III, and Fig. 17, the etch rate of the titanium-rich ($\text{Ti}_{50}\text{Ta}_{50}$ alloy) sample is less than that of the sputtered TiSi_2 or the CVD-deposited TiSi_2 , while the tantalum-rich ($\text{Ti}_{10}\text{Ta}_{90}$) sample is greater than pure TaSi_2 . These differences may be attributed to the presence of titanium-rich compounds such as Ti_5Si_3 and TiSi_2 in the Ti-rich sample, and lower TaSi_2 contents of the $\text{Ti}_{10}\text{Ta}_{90}$ alloy sample.

D. Discussion

These investigations were started hoping that during the interaction between Ti-Ta mixtures and silicon or polysilicon, a phase separation of TiSi_2 from TaSi_2 would lead to the formation of TiSi_2 at the silicon surface and TaSi_2 on the outer region. A reaction between the substrate silicon with a refractory-metal-noble-metal alloy mixture¹¹⁻²¹ leads to the formation of the noble-metal silicide on silicon and to the accumulation of the refractory metal (or the silicide formed at the higher temperatures) at the top. However, we did not observe this type of phase separation as is clear from the Auger analysis results of Figs. 9-12; both Ti and Ta are present throughout the film thickness. This resulted in the poor etch stability of the reacted films—mainly due to the presence of TiSi_2 .

The absence of phase separation in this system could be associated with the closeness of the first silicide formation temperatures for Ti on Si and Ta on Si. The reaction temperatures are reported in the range of 500–600 °C and 550–600 °C for the two systems, respectively. In noble-metal/refractory-metal systems, the noble-metal/silicon reaction occurs at very low temperatures (~200–300 °C) compared to the refractory-metal/silicon case (≥ 500 °C). Also, the presence of small amounts of oxygen in these alloy systems may have had an influence on the interaction behavior. Whether this influence of oxygen on the reactions would inhibit the phase separation is not known and the data presented in this paper are insufficient to address this point further. Titanium is difficult to work because it absorbs oxygen readily and the appearance of the Ti_5Si_3 or the Ta_5Si_3 phases after low-temperature anneals could be impurity stabilized. The impurity may be oxygen or it may be the presence of the other refractory metal.

Finally, the etch rate of the ternary silicide alloy on polysilicon is higher than on silicon. This is possibly due to: (a) smaller grain size of the silicides on polysilicon and (b)

phosphorus from the polysilicon which is known to redistribute and dissolve into the silicide during the silicide formation anneals.²²

V. SUMMARY

The formation of disilicides of titanium and tantalum from Ti-Ta alloys codeposited on silicon and polysilicon have been investigated using x-ray diffraction techniques, resistance measurements, etch rate measurements, and Auger electron spectroscopy. Titanium and tantalum in the Ti-Ta alloy interacted separately with silicon, in the same temperature range, without any interaction between the two metals. The initial reaction was observed after the 600 °C, 30-min anneal. The stable end-phase formed at temperatures ≥ 800 °C are TiSi_2 and TaSi_2 . High molecular weight intermetallics, such as Ta_5Si_3 and Ti_5Si_3 that are normally not detected in Ta-Si and Ti-Si interaction studies, were detected, suggesting a stabilizing effect from impurities or the other refractory metal. The sheet resistance and the etch rate in BHF of the heat-treated samples are a strong function of the titanium content of the Ti-Ta alloy. Since no phase separation occurred, the protection of TiSi_2 from covering TaSi_2 did not result.

ACKNOWLEDGMENTS

Authors would like to thank H. J. Levinstein for suggesting this study, E. Lane for Auger analysis, and J. Fink for film depositions.

- ¹S. P. Murarka, D. B. Fraser, A. K. Sinha, and H. J. Levinstein, *IEEE J. Solid State Circuits* **SC-15**, 474 (1980).
- ²J. M. Harris, S. S. Lau, M. A. Nicolet, and R. S. Novicki, *J. Electrochem. Soc.* **123**, 120 (1976).
- ³S. E. Bobcock and K. N. Tu, *J. Appl. Phys.* **53**, 6898 (1982).
- ⁴K. N. Tu and J. W. Mayer, in *Thin Film—Interdiffusion and Reactions* (Wiley, New York, 1978), p. 359.
- ⁵C. A. Osborn, M. Y. Tsai, S. Roberts, C. J. Luccese, and C. Y. Ting, in *VLSI Science and Technology, 1982*, edited by C. J. Dell'Oca and W. M. Bulle's (The Electrochemical Society, Princeton, NJ, 1982), p. 213.
- ⁶A. Appelbaum, M. Eizenberg, and R. Brenen, *J. Appl. Phys.* **55**, 914 (1984).
- ⁷K. N. Tu, *J. Vac. Sci. Technol.* **19**, 766 (1981).
- ⁸S. P. Murarka and D. B. Fraser, *J. Appl. Phys.* **51**, 1593 (1980).
- ⁹S. P. Murarka and D. B. Fraser, *J. Appl. Phys.* **51**, 342 (1980).
- ¹⁰S. P. Murarka, *Thin Solid Films* **140**, 35 (1986).
- ¹¹K. N. Tu, *J. Vac. Sci. Technol.* **19**, 766 (1981).
- ¹²S. Thomas and L. E. Terry, *J. Appl. Phys.* **47**, 301 (1976).
- ¹³J. O. Olowolafe, M. A. Nicolet, and J. W. Mayer, *J. Appl. Phys.* **47**, 5182 (1976).
- ¹⁴R. Pretorius, J. O. Olowolafe, and J. W. Mayer, *Philos. Mag. A* **37**, 327 (1978).
- ¹⁵T. G. Finstad and M.-A. Nicolet, *J. Appl. Phys.* **50**, 303 (1979).
- ¹⁶J. W. Mayer, S. S. Lau, and K. N. Tu, *J. Appl. Phys.* **50**, 5855 (1979).
- ¹⁷J. O. Olowolafe, K. N. Tu, and J. Angilello, *J. Appl. Phys.* **50**, 6316 (1979).
- ¹⁸K. N. Tu, W. N. Hammer, and J. O. Olowolafe, *J. Appl. Phys.* **51**, 1663 (1980).
- ¹⁹M. Eizenberg, G. Ottoviani, and K. N. Tu, *Appl. Phys. Lett.* **37**, 87 (1980).
- ²⁰R. Thompson, M. Eizenberg, and K. N. Tu, *J. Appl. Phys.* **52**, 6783 (1981).
- ²¹G. Ottaviani, K. N. Tu, J. W. Mayer, and B. Y. Tsaur, *Appl. Phys. Lett.* **36**, 331 (1980).
- ²²A. H. Van Ommen, H. J. W. Houtum, and A. M. L. Theunissen, *J. Appl. Phys.* **60**, 625 (1986).